Cable Connector Profile Measurement Using Laser Light Plane Sectioning

John Hayes[1], Markus Leitner[2], Paul O'Leary[3]
Ronald Ofner[4], Christian Sallinger[5]
Department of Automation, University of Leoben
Peter-Tunner-Str. 27, A-8700 Leoben
Tel. ++43 3842 402 - 9031, Fax - 9032
Email: automation@unileoben.ac.at

August 25, 2000

[1]Tel. ++43 3842 402 - 9047, Email: john.hayes@unileoben.ac.at
[2]CD-Labor fuer Sensorische Messtechnik, Tel. ++43 3842 402 - 9046, Email: markus.leitner@unileoben.ac.at
[3]CD-Labor fuer Sensorische Messtechnik, Tel. ++43 3842 402 - 9031, Email: automation@unileoben.ac.at
[4]Tel. ++43 3842 402 - 9047, Email: ronald.ofner@unileoben.ac.at
[5]Tel. ++43 3842 402 - 9047, Email: christian.sallinger@unileoben.ac.at

Contents

Chapter 1

Introduction

This report presents the results of an experiment designed to test a prototype integrated optical-robotic measurement system that is intended to measure the external profile of arbitrarily shaped cable connectors. The task of the measurement system is to determine the 3-dimensional geometry of the external features of the cable connectors for subsequent manufacture of a jig to hold the connectors accurately in place during an automated cable-tree assembly and wiring process.

The measurement of 3-dimensional objects requires 6 degrees-of-freedom (DOF). The overall measurement task has been decomposed into multiple 2-dimensional tasks. We impose some constraints enabling us to obtain measurements of planar cross-sections of the connector using only 1 DOF of the robot. However, to attain the necessary initial assembly configuration prior to making the first measurement, all 6 DOF are required. Once the first cross-section measurement data has been obtained, 5 DOF are required to move to the start position for the next section.

Integrating an industrial robot into the measurement system has the advantage that the measurement procedure can be automated. The main disadvantage is that accuracy, repeatability and calibration issues must be addressed. We have designed the measurement procedure, carried out by the robot, to be less dependent on absolute robot accuracy and instead rely on the lower limits: repeatability and relative accuracy. By minimizing the DOF used by the robot at key stages in the process, we remain closer to the lower limits of the robot accuracy.

The robot used in the measurement system is a KUKA KR-15/2 with a manufacturer stated repeatability of ± 0.1 mm. Relying on the results from

an earlier study [1], we can reach a repeatability of ± 0.025 mm. This is done by taking heat-up effects of the robot into consideration.

The measurement head is a custom design from the Institute for Automation at the University of Leoben. It employs the concept of laser light plane sectioning. A laser diode fitted with line optics creates a light plane. The laser plane intersects the connector. The trace of the intersection is visible and a CCD camera records its image. Knowing the relevant camera parameters and laser light plane equation, the Euclidean distances from a reference point on the laser plane to points on the trace can be measured. After calibrating the camera and knowing the robot motion geometry, the images are rectified into a true planar cross-section of the connector. The rectified image data are then filtered with an FFT procedure. The result is a closed planar curve representing a cross section of the connector. The planar sections are stacked on an axis determined during the calibration, giving an image of the reconstructed cable connector. A solid model of the connector is then obtained in MATLAB using solid modeling functions.

Chapter 2

Apparatus and Procedure

2.1 Objective and Apparatus

The objective of the experiment is to test a novel procedure for using an integrated robotic optical measurement system to determine the scaled external profile features of arbitrarily shaped cable connectors within a certain, though as yet unspecified, range of dimensions. The desired measurement error tolerance is ±0.1 mm.

2.1.1 Robot

The custom measurement head, see Section 2.1.2 was mounted to a KUKA KR-15/2. It is a *wrist-partioned* [2] robot with six actuated revolute axes. The axes, together with the base and tool reference coordinate frames, are illustrated in Figure 2.1. Its rated payload is 15 kg and the volume of its working envelope, using the wrist-centre (intersection of orthogonal axes 4, 5 and 6) as reference point, is approximately 13.1 m^3. Detailed specifications are available on-line from http://www.kuka.de/web/re_engl/index.html. The most important specification related to this experiment is the manufacturer stated repeatability:

$$\text{stated repeatability} \quad = \quad \pm 0.1 \text{ mm}.$$

In a separate investigation we have determined that this value may be overstated. That is, we have discovered that the robot repeatability is de-

[2] Wrist-partitioning means axes 4, 5 and 6 all intersect in the same point, so positioning tasks are decoupled from orienting tasks. Hence the term *partitioned*.

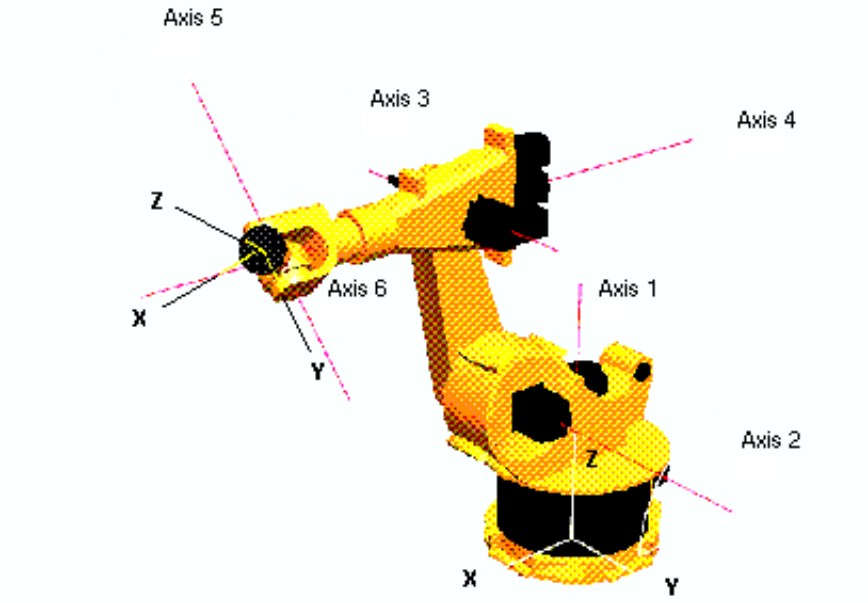

Figure 2.1: KUKA KR-15/2.

pendent upon operating temperature in addition to dimensional tolerances, controller kinematics computations, and dynamics [1]. If the task can be implemented in a way that respects this dependency, the repeatability of the robot, at least in principal, can be improved by nearly an order of magnitude. For instance, when only thermal effects are taken into account, the repeatability can be improved to [1]:

$$\text{thermally compensated repeatability} \quad = \quad \pm 0.025 \text{ mm}.$$

When other factors, such as dynamics, are compensated for the repeatability may still be improved. Since the repeatability of a robot lower bounds its accuracy, the implication is that measurement tasks requiring accuracy of ± 0.1 mm can be carried out by a measurement system that integrates a standard industrial robot, such as the KUKA KR-15/2. There may be no real need to invest in a higher precision robot, such as the Stäubli RX60 or ABB RB 140 series of precision robots[3]. There are of course constraints, but the difference in cost may be worth the additional task planning.

[3]In the absence of experimental data carried out with Stäubli and ABB robots, we can only compare manufacturer catalogue specifications to those of the KUKA.

2.1.2 Measurement Head

The measurement head is one designed and built by the Institute for Automation, University of Leoben. It uses a laser fitted with line optics and a CCD camera. The camera and laser are inclined at 45° relative to each other. Moreover, the head is mounted to the robot tool flange such that the axis of symmetry of the camera and laser is incident on axis 6 of the robot. Figure 2.2 shows the mounted head in position to produce measurement data. Table 2.1 lists the components used to obtain the raw measurement data for this experiment.

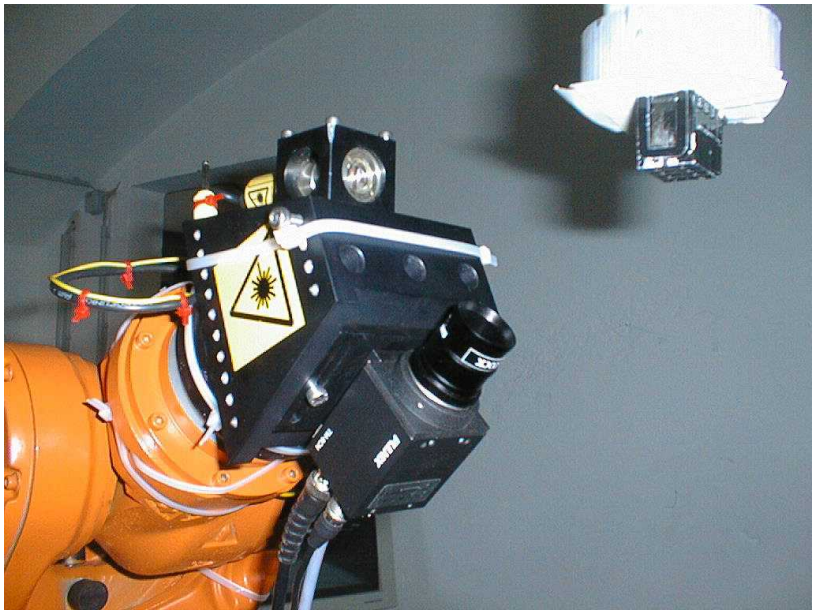

Figure 2.2: Measurement head mounted to KUKA KR-15/2.

Table 2.1: Measurement head components.

CCD-Camera	Pulnix TM-6CN	CCIR-Norm Resolution: 752(H)x582(V) Cell size: 8.6(H)x8.3(V) μm
Camera Optics	Rodenstock	Aperture = 1:4 Focal Length = 15 mm Magnification = 0.14×
Laser Diode	Schaefter and Kirchhoff	Wavelength = 638 nm Max. output power = 11 mW
Laser Optics		Line optics
Framegrabber	National Instrument	PCI-1408 monochrome

2.2 Procedure

The required measurement information for creating a scaled reconstruction and solid model of the exterior features of a cable connector between the planes perpendicular to the pin ends and the wire input portal is obtained by stacking a series of horizontal sections of the connector. The sections are obtained by projecting a laser plane onto the connector. The trace of the plane on the connector is viewed by the camera. Since there will always be some invisible features when seen from any particular vantage point, more than one view is necessary. It is our assumption that 8 views in the plane of the section are sufficient. The images are rectified and the result is a planar section of connector yielding all external profile features.

The measurements all take place ideally, but not necessarily, about the axis of rotation of joint 1, axis 1 (see Figures 2.1 and 2.3). Once an initial robot assembly configuration is attained, the measurements for an entire section (i.e., the trace of the object being measured in the plane of the laser line) can be obtained. The plane of the laser line is chosen to be, and remains, parallel to the xy-plane in the robot base frame, illustrated in Figure 2.1.

Work pieces are mounted in a fixture, see Figure 2.3, such that their longitudinal axis is perpendicular to the plane of the laser line, illustrated in Figure 2.4. The laser diode light source is considered to be a point, P. The projected laser line, created with the line optics, is a line that does not contain P. The laser plane is determined by the line and point P.

Figure 2.3: Measurement frame axis and joint axis 1 are parallel.

2.2.1 Initial Position

The initial robot assembly configuration is selected so that it fulfills the following criteria.

1. The laser plane is parallel to the xy-plane of the base frame.
2. The trace of the laser plane on the work piece is near the interface between the work piece and fixture, as in Figure 2.5, although the position shown is not the initial one.
3. The image is within the field of view of the camera.

These criteria can be achieved independently of the first joint axis. Indeed, only 5 DOF are required: one to position and two to orient the plane; two to adjust the view point of the camera. Since the initial configuration is independent of joint axis 1, we are free to choose any value for that joint angle.

Note: We refer later to the robot *links*. Joint 1 permits rotation about axis 1, shown in Figure 2.1. It joins the first link to the *zeroth* link, the relatively fixed base of the robot. Joint 2 connects links 1 and 2, joint 3

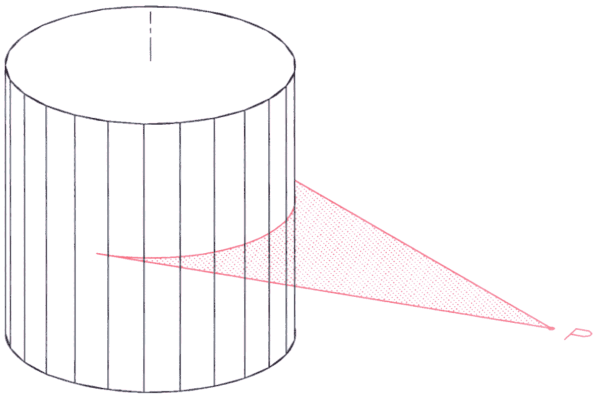

Figure 2.4: The laser light plane is perpendicular to longitudinal axis of the object.

connects links 2 and 3, etc.. In general, the n^{th} joint connects the $(n-1)^{st}$ to the n^{th} link, permitting relative rotation between the neighbouring links about axis n.

2.2.2 Degree-of-Freedom Matching

The goal of each measurement is to obtain a segment of a planar section of the connector. This means that the measurement task requires, at most, 3 DOF. The robot has 6. Which should be used in obtaining multiple views of the section so that a composite image of the entire section can be reconstructed from the segments? By constraining the plane of the sections to be parallel to the principal xy-plane of the base, we eliminate 1 DOF. Moving the measurement head in a circle with a fixed radius, centred on the joint axis 1 eliminates another. Thus, once the initial assembly configuration has been established, only motions about joint axis 1 are required to obtain enough images for reconstructing a complete composite image of the section.

2.2.3 Measurement Sequence

As previously mentioned, the value for joint angle 1 is arbitrary. We select the first position to be Pos. $1 = -180°$ in the xy-plane of the base, using the

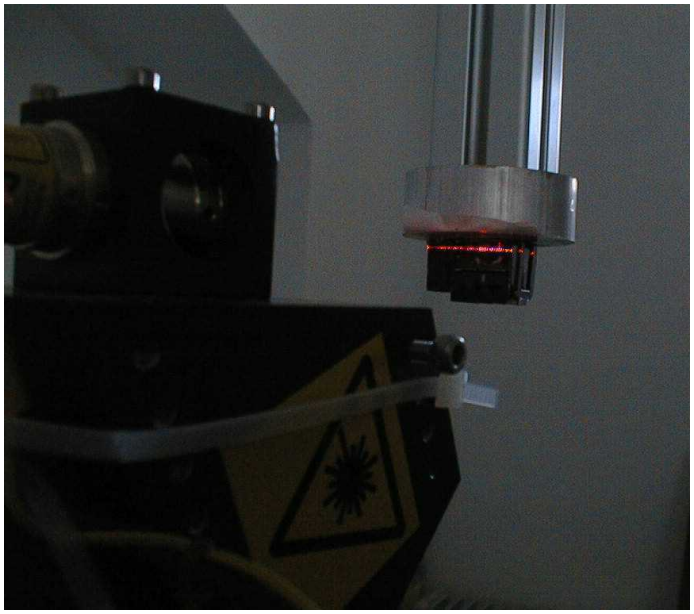

Figure 2.5: Trace of the laser light plane on a work piece.

left-handed angle measurement employed by the robot controller. No image is recorded in this position. Subsequent positions are at $+45°$ increments. This gives 9 positions around a circle centred on the z-axis. The first and last positions have the same joint angles. Images are recorded in positions 2 through 9. This is a programming oversight, in the future measurements will be made in positions 1 through 8. Position 9 can be omitted.

This gives 8 views of the laser light plane trace on the connector. We believe this number to be sufficient for assembling a composite image of a planar section of the connector. Data with the highest confidence interval can be selected from adjacent images containing overlapping segments. We have developed a linear criterion for computing the confidence interval, although this has not yet been implemented.

Once all 8 views of a section have been obtained the laser light plane is moved an incremental distance in the negative z-base frame axis direction and 8 more images are recorded. This process terminates when the distal end of the connector has been reached. The overall length of the connector is known a priori. However, it would present no difficulty, in principal, to detect the connector ends from raw images because there would be no laser plane trace visible in the field of view of the camera in all 8 positions. The z-axis increment and number of sections are determined from this knowledge.

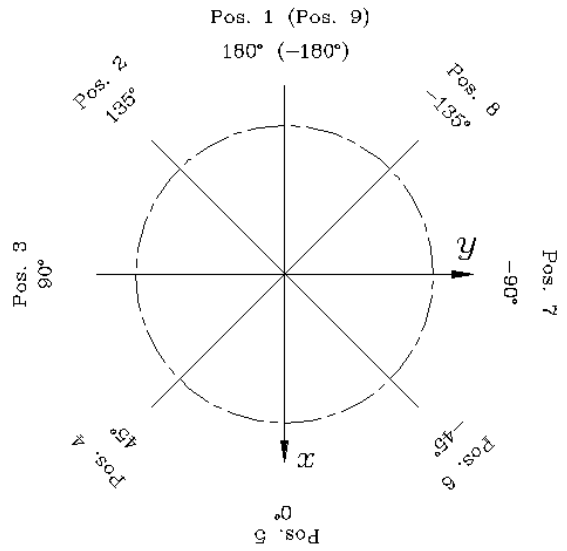

Figure 2.6: Position sequence for measuring one section.

The process of of recording images is automated via LabVIEW, permitting communication between the KUKA controller PC and a separate PC containing the framegrabber.

2.3 Measurement System Calibration

Once all required images have been recorded, they must be used to construct a solid model of the workpiece. To do this, we require precise position and orientation information on the measurement head. This involves a calibration procedure for the measurement system to identify all the parameters required to determine the transformations needed to rectify the images. There are two main approaches:

1. *Open-loop methods.* Most proposed methods require an external metrology system for parameter identification [2]. Individual poses of the robot are attained by moving all the joints. The kinematic parameters are estimated from some form of nonlinear optimization of the entire set of poses [3].

2. *Closed-loop methods.* The robot end-effector is attached to a grounded calibration fixture. This forms a mobile closed kinematic chain [2]. Calibration is achieved using joint angle sensing output without any external metrology system. The endpoint constraints may vary from 6 to 1 motion constraints [4]. A variation of this approach uses a grounded laser interferometer and a reflector mounted to the robot end-effector. No physical constraint is involved, but if the interferometer is rigidly fixed to ground, it may be thought of as closing the kinematic chain [5]. Parameter identification is estimated using nonlinear optimization as for open-loop methods.

Our approach may be classified as a closed loop method. First, a calibration object is measured using the same set-up fixture and robot motions as for the connector, see Section 2.4.1. Here we assume that by requiring only joint axis 1 to move, the relative error from pose-to-pose should be acceptably small. Moreover, small deviations in this joint angle will produce correspondingly small position errors because the radius of the circle traversed by the measurement head is small compared to the link lengths. Our conjecture is that we implicitly obtain a linear first order calibration estimation of the laser plane virtual reference point with respect to the robot wrist point. At this point it is only a conjecture, and more work needs be done for verification. What remains is to calibrate the camera to eliminate image distortion. This will be discussed in the next section.

2.4 Camera Calibration

We assume there are two predominant sources of error introduced by the camera used to view the laser plane trace: perspective distortion caused by the projection of the trace onto the plane of the CCD chip and; distortion determined by the construction of the lens. Perspective and the linear portion of the lens distortion can be compensated using the same algorithm [6].

A calibration grid of known dimensions is required. All recorded laser traces lie in the laser plane. The camera is calibrated by superimposing the plane of the calibration grid on the laser plane, see Figure 2.7 a). Employing some elementary projective geometry allows for the computation of a homogeneous transformation which can be used to map points, known in the image plane of the camera, see Figure 2.7 b), to the corresponding points on

the known calibration grid. See [6] for a detailed explanation.

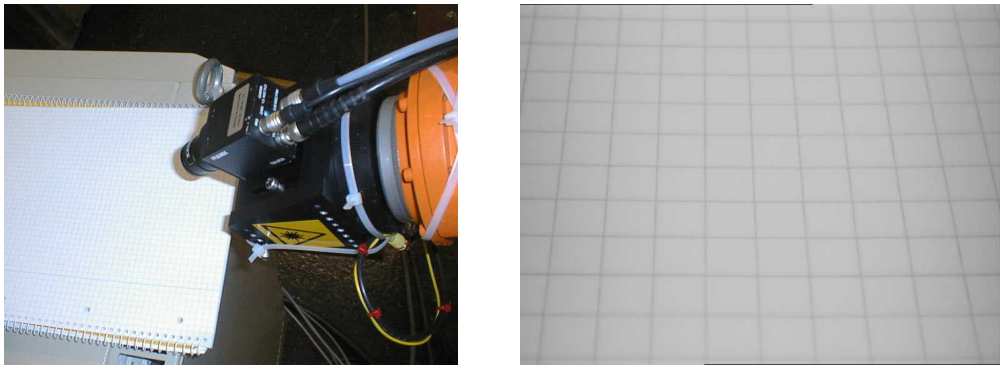

Figure 2.7a) Camera and grid; b) Camera view of grid.

The result of the computation is a transformation matrix that is used to eliminate the camera distortion in the laser plane. In effect, this projects the image of a laser plane trace from the projective image plane to an Euclidean plane. We can reassemble the plane traces into a planar section of the connector in this Euclidean plane, and can extract measurements from it.

The transformation matrix needs to be computed just once for the head. Only the coordinates of the points of the laser trace in the image have to be multiplied by this matrix. For a typical image this involves 400-600 matrix multiplications, see Section 2.4.1. This is computationally efficient compared to multiplying all pixels of a raw image, which would involve more than 300,000 matrix multiplications.

2.4.1 Rectifying Planar Section Image Data

Once the transformation needed to remove lens distortion has been computed, we can proceed to rectify the image data and build an approximate solid reconstruction of the connector by stacking planar sections. To suitably condition the raw data for each section the following steps are required.

1. Determine a discrete set of point coordinates for each laser plane trace segment. This is done by first determining the best *path* through the

raw image using a suitable *centre-of-gravity* (COG) algorithm, see [7].

2. Each point set is then mapped to the Euclidean plane using the transformation obtained from the camera calibration procedure.

We now require a suitable longitudinal axis upon which we can reassemble the 8 segments in one planar section, then stack the planar sections. The *reconstruction* axis is determined using a calibration cylinder, with roughly the same cross-section area as the connector, see Figure 2.8.

Figure 2.8: Cylindrical calibration object and cable connector.

The following steps are now required.

3. The raw image data of the plane traces on the cylinder are conditioned as above. We obtain a rectified coordinate set referred to some planar reference frame. **Note:** for this experiment we used only one planar section of the cylinder. The assumption was that cylinder longitudinal axis was parallel to joint axis 1. All layers of the cable connector will be referenced to the appropriate view of the cylinder section segment.

4. The centres of the camera-distortion compensated arcs are determined using an improved version of the algorithm found in [8].

5. Translate the coordinates of the camera-distortion compensated connector segments so the arc centre coordinates are the reference frame origin.

6. Rotate the new coordinates to remove the rotation angle of the first joint angle. **Note:** We cannot directly combine the two transformations into a homogeneous transform because the first is a coordinate transformation while the second is a geometric one. While this slows the computation it is preferred over the introduction of additional transformation arithmetic, making the programming more intuitive and easier to follow.

Using the cylinder section centre translation offsets and the robot angle offsets, we reconstruct the connector segments in the appropriate laser plane (z = constant). Figure 3.2 illustrates both the calibration cylinder and connector in the measurement frame for corresponding robot measurement positions.

Chapter 3

Results

The cable connector used in the experiment, shown in Figures 2.8 and 3.7, had a length of 24 mm. We decided that to demonstrate the validity of our approach obtaining 20 planar sections with a 1 mm separation would suffice. That is, the z-axis increment is 1 mm. The images obtained from the measurement positions in each section, repeated in Figure 3.1 for convenience, were assigned file names in the way listed in Table 3.1.

Table 3.1: Measurement position file names.

Measurement Position	File Name
Pos. 2	A_n
Pos. 3	B_n
Pos. 4	C_n
Pos. 5	D_n
Pos. 6	E_n
Pos. 7	F_n
Pos. 8	G_n
Pos. 9	H_n

where the subscript n varies as $\{0, 1, 2, \ldots, 19\}$, representing the z-increment index. The plane associated with $n = 0$ is 19 mm distant from that of $n = 19$.

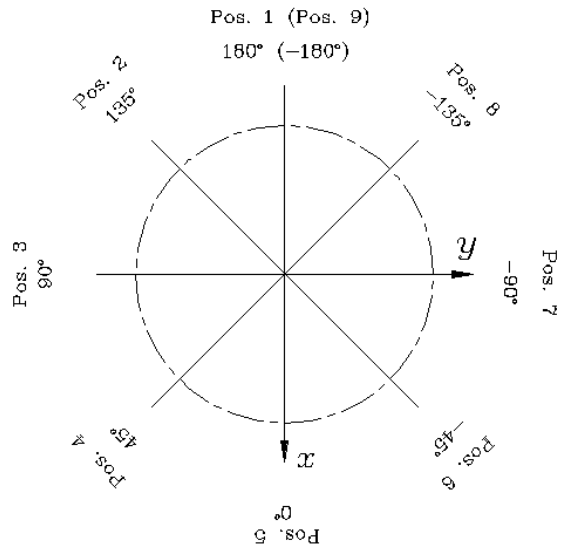

Figure 3.1: Position sequence for measuring one section.

3.1 Obtaining Raw Images

We measured 20 different planar sections of the connector taking 8 images in each plane, for a total of 160 images. The first plane was near the measurement frame-connector interface. The remaining 19 sections were at 1 mm increments in the negative z-axis direction.

Only 1 planar section of the calibration cylinder was measured. Each of the 8 segments was used to condition the data for the corresponding connector segment. Note, the 8 different colours in each section represent the 8 different segments which correspond to the 8 distinct views of the object, see Figures 3.4 and 3.5.

3.2 Image Rectification and Section Reconstruction

Using the computation steps listed in Section 2.4.1, MATLAB programmes were written to rectify and reconstruct each section of the connector. The calibration cylinder section was also reconstructed: the mean radius of the 8 segments is $R = 24.2797$ mm, while the standard deviation is $\sigma = 0.0413$.

Shown in Figure 3.2 are the cylinder and cable connector in the measure-

ment frame with the robot in position A_0, while Figure 3.3 shows the raw camera images. Figures 3.4 and 3.5 are the MATLAB reconstructions of the cylinder cross section and the cable connector section in layer 0, respectively. Note that in the raw images there are some outliers. The resulting unwanted data can be trimmed from the data set by eliminating the first and last 10% of data points in a segment; and eliminating data with an excessively steep slope, e.g. greater than 60°. However, this step is yet to be implemented.

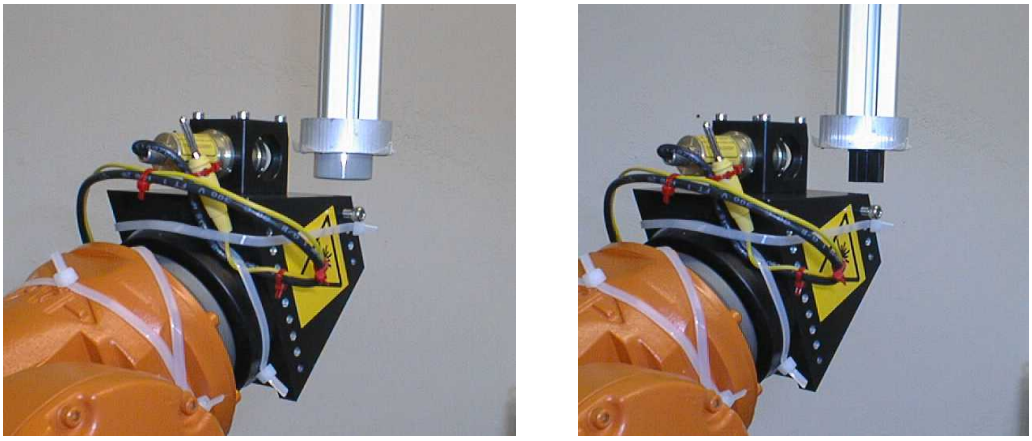

Figure 3.2: Calibration cylinder and cable connector in measurement frame. The robot is in position A_0.

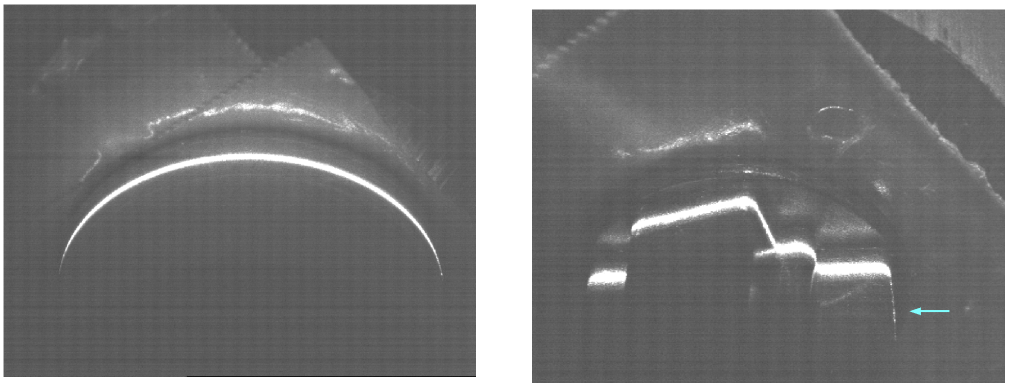

Figure 3.3: Camera view of laser plane trace on cylinder and cable connector from position A_0. The blue arrow points towards data points with excessively steep slope.

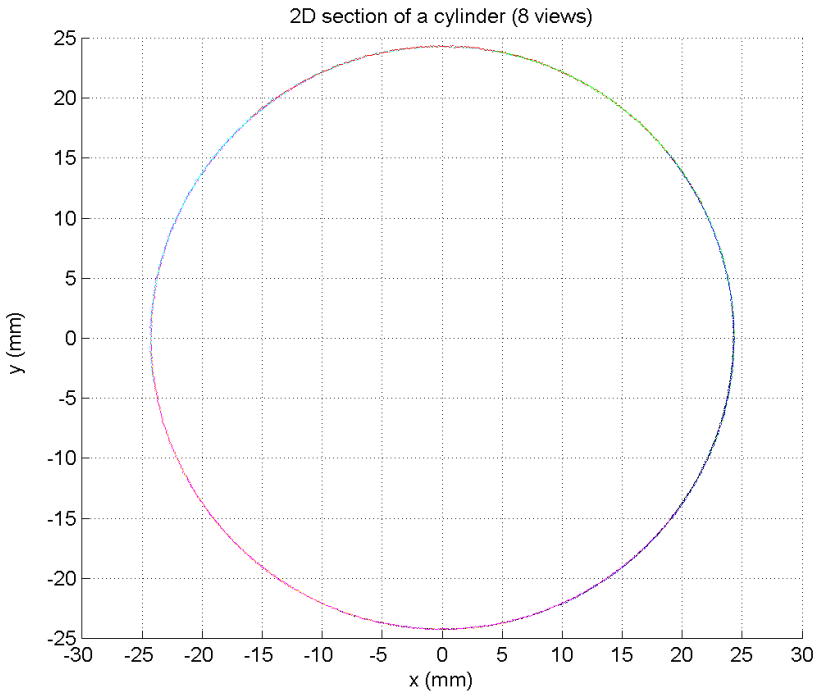

Figure 3.4: Reconstructed calibration cylinder section.

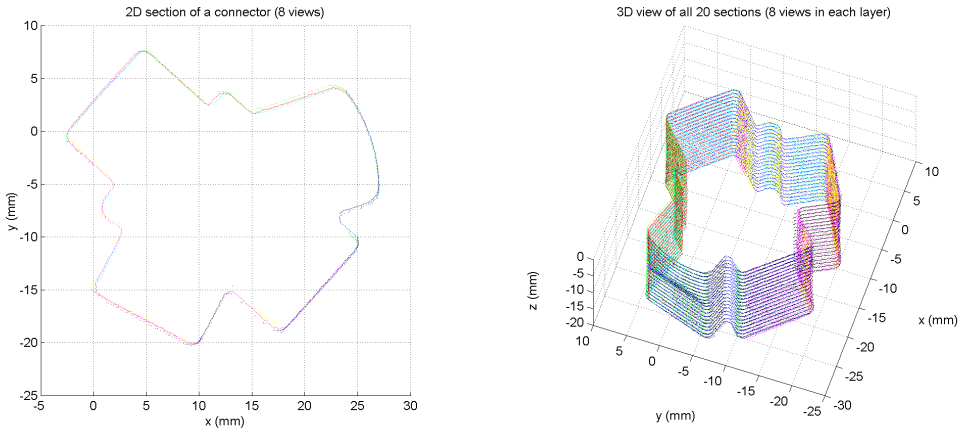

Figure 3.5: Reconstructed cable connector section in layer 0; 3D view of all sections.

3.3 Data Filtering

Two preliminary data filtering methods have been tested, without outlier removal. They are a 2D Butterworth filter and Fourier elliptical descriptors. We believe the latter method to be superior since FFT with efficient implementations are available in most programming environments. Figure 3.6 shows a first implementation of the filter applied to the data from all 8 segments in the zeroth section were concatenated into one long data set. The result is the FFT filtered profile shown in Figure 3.6, the red circle indicates the start point of the curve.

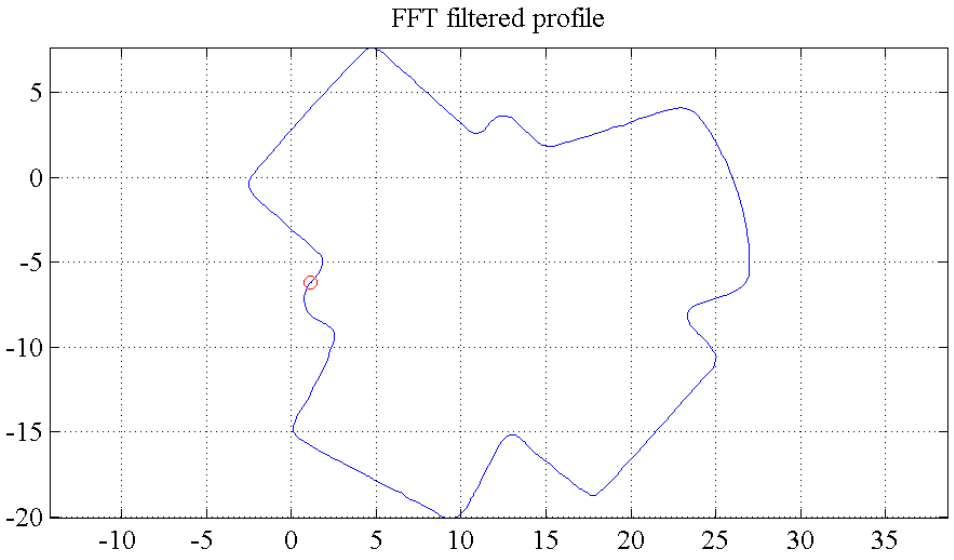

Figure 3.6: FFT filtered profile layer 0.

3.4 Solid Model

The next step is to integrate the solid reconstruction obtained by stacking the sections into a solid model of the connector. A solid model is the unambiguous and complete mathematical representation of the shape of a 3-dimensional physical object in a form that a computer can process [9]. Solid modeling is an essential element necessary for creating and communicating shape information. The 20 planar sections of the cable connector stacked on the appropriate axis in the appropriate planes z=constant do not constitute

a solid model. This is because the sections are constructed of discrete sets of measured points. They are not the output of a mathematical model which unambiguously and completely describes the connector. In order to proceed, we require a greater understanding of the topology and geometry of solid reconstructions, as the one shown in Figure 3.5.

We proceed as follows. The data of individual segments in each layer are filtered using the FFT procedure. Thus, the data in the 8 segments in a section are seamlessly joined, and modelled mathematically, see Figure 3.6. Using MATLAB, the 20 layers of the FFT filtered data can be used to create a solid model. Figure 3.7 shows the connector itself, while Figures 3.8 and 3.9 are a wireframe and rendered solid model, respectively.

Figure 3.7: Cable connector.

3.5 Discussion

Given all the approximations and roughly constructed and calibrated tools used in this experiment, we see the method is fairly robust. Inspection of Figure 3.5 reveals an excellent planar cross section reconstruction of the cable connector that is very true to the actual features, despite the noise in the rectified data. Figure 3.5 suggests we are on the right track in the development of this apparently novel technology. There appears to be little, or no shearing of adjacent sections with respect to the z-axis. This is with absolutely no data filtering.

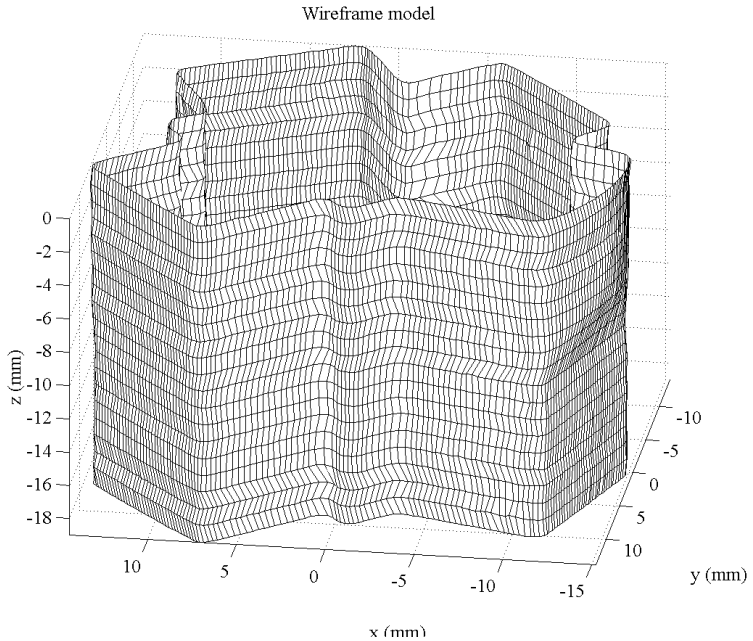

Figure 3.8: Wireframe model.

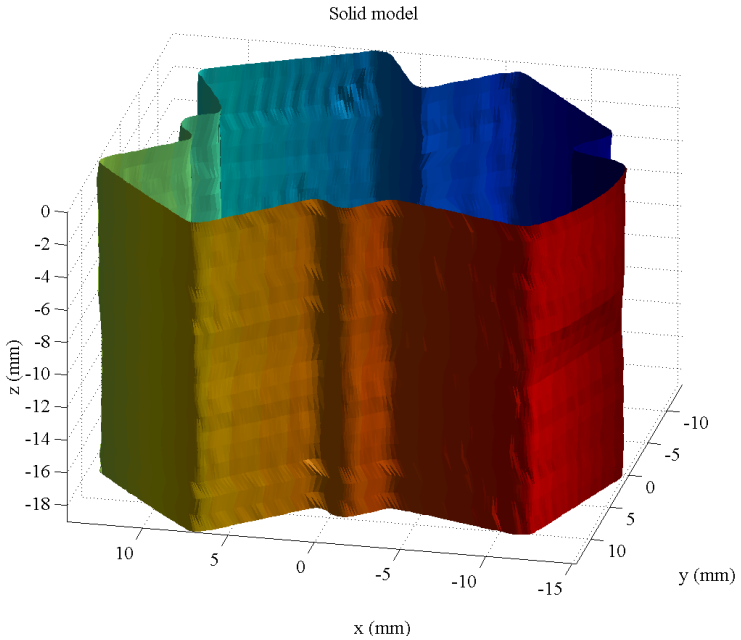

Figure 3.9: Rendered solid model.

Some miss-alignment between certain segments is evident in the planar reconstruction illustrated in Figure 3.5. We attribute this to two main causes. First, to camera plane data points with excessively steep slopes. A small blue arrow in 3.3 points towards one such point set on the lower right-hand corner of the cable connector trace. Second, to the coarseness of our camera calibration.

In the cylinder section reconstruction, Figure 3.4, there is a scaling problem. The dimensions on the y- and x-axes are millimeters (mm), and the dimensions of the section should be able to be scaled directly from the figure. However, the actual cylinder diameter is 43 mm, while the reconstructed section has a diameter of 48.5594 mm, determined from the mean radius of the 8 segments. This discrepancy can also be attributed to camera calibration. Table 3.2 lists the calibration cylinder section data.

Table 3.2: Calibration cylinder section data.

No. Segments	Actual Radius, R_a	Mean Radius, R_m	Std. Dev., σ
8	R_a=21.5 mm	R_m=24.2797 mm	σ=0.0413

Here we have the possibility to use a linear scaling factor on the connector dimensions in a section. Since the cylinder dimensions are known a priori, the scaling factor is easily obtained. It may not be needed if the camera calibration is refined, but is expressed by the dimensionless ratio:

$$f_{cyl} = \frac{R_a}{R_m}. \tag{3.1}$$

The vertical scaling is independent of the above considerations. We have assigned exact nominal values to the z-axis coordinates on our MATLAB routines, assuming the relative positioning accuracy along this axis to be sufficient. However, we have no empirical evidence, as yet, to support this assumption. In a separate study, we are investigating the relative positioning accuracy of some industrial robots, including the KUKA KR-15/2. We will soon be able to assess the vertical reconstruction accuracy.

Examining the solid connector reconstruction shown in Figure 3.5, one can immediately recognise the shape as that of the cable connector shown in Figure 3.7. To achieve greater reconstruction resolution more planar sections are required. Here the question of relative positioning accuracy of the robot

immediately presents itself. The reconstruction elevation accuracy depends on the relative positioning accuracy along the z-axis of the robot.

The wireframe and solid models in Figures 3.8 and 3.9 are also quite true to the external features of the connector (Figure 3.7). The *zig-zag* patterns in the wireframe are the result of each section having a different number of points. The *artifacts* in the image are due to the fact the outlier data has not been filtered. The same comments hold for the rendered solid model of the wireframe, Figure 3.9. Here the effects are somewhat more dramatic visually, but will be mitigated, perhaps eliminated, with suitable raw data filtering.

Chapter 4

Conclusions

Results from this experiment indicate that it is possible to measure external features of complicated shapes using the light sectioning technique combined with robot generated motion. Moreover, the results suggest our procedure is a suitable tool for constructing solid models for CAM purposes.

Visual inspection of the reconstructed sections, Figure 3.5, and the solid model, Figures 3.8 and 3.9, and comparing to the physical connector, Figure 3.7, reveals the procedure we have developed can produce a solid model acceptably complete in desired external detail.

The vertical accuracy depends on the relative positioning accuracy of the robot along the z-axis of the base frame. We assume the accuracy is sufficient for our purposes at present. The important observation is that there appears to be little, or no shearing of the stacked planar sections with respect to the z-axis. This indicates that the cylinder axis is suitable for a stacking axis. The next step is to determine error bounds on the dimensions of the solid model. However, we believe the more *difficult* problem of actually obtaining and processing the image data has been solved with our procedure.

The robot measurement system calibration designed for this particular measurement task succeeds in identifying the needed kinematic parameters. However, the procedure is atypical in that the parameters are obtained implicitly, exploiting the invariant features of the calibration cylinder. By this we mean the cylinder axis and radius are used for reference to derive the information necessary to reconstruct the 8 segments in a section from the raw data. We are becoming more-and-more convinced that the need for *absolute calibration* of the robot is artificial. Since the movements of a robot from one position to another are always relative to the first position, it may be

that a simpler relatively accurate robot calibration may be all that is necessary. However, this is purely conjecture at the moment. Work carried out in parallel studies will yield empirical data with which the conjecture can be examined in objective detail.

We conclude that these results show that an integrated robotic optical measurement system can be set up to measure cable connector external solid geometry. Until we have implemented a raw image data filter, no measurements will be made. This, for the simple reason that the data is, as yet, too noisy to obtain stable dimensional tolerances. Due to this, we can assign no value to the dimensional accuracy of our solid model. This notwithstanding, we have good reason to believe that the required tolerance of ± 0.1 mm can be attained in the automated measurement and manufacture of cable connector jigs.

Chapter 5

Suggestions for Future Work

The goal of this experiment was to determine if our procedure is, in principle, feasible. Because of this relatively large tolerances were given to calibration and no confidence interval was used to trim data. Order-of-magnitude improvements in the overall measurement accuracy will be achieved by refining the camera calibration tools and calibration data acquisition. Additional improvements will be obtained by implementing some form of confidence interval data trim. This can be attained by eliminating the first and last 10% of the data points in a segment, removing outliers and data with an excessively steep slope. Clearly, raw image lines with slope greater that 45% will be better viewed from an adjacent measurement position, i.e., $\pm 45°$.

We can mitigate the effects of excessively steep slopes by computing a confidence interval for the image points. The steeper the slope between two neighbouring points in the non-rectified image, the lower the the confidence that the second point represents *good* data. This inverse relationship is linear and simple to implement. Thus, only data within a predefined confidence interval will be passed on for reconstruction and FFT data filtering.

So far, we only have a rough idea of the measurement error tolerance in each planar section of the connector. The aforementioned improvements will apply only to this measure. The vertical error tolerance must be determined by assessing the relative positional accuracy of the robot along the z-axis. A separate study to this effect is underway. Additionally, a way to quantify shearing with respect to the z-axis must be established.

Calibration must be considered in greater detail. Using the right circular cylinder (see Figure 2.8), the laser plane and camera allows us to form a kinematic chain that is closed via the camera view of the laser plane trace

on the cylinder. We can then write closure equations in terms of the joint angles and link lengths, including the measurement head kinematic parameters. The joint angles can be read directly from the joint resolver output. For n different views of the cylinder, we obtain n different sets of equations. With a sufficiently large n we obtain an overconstrained system of non-linear equations in terms of the kinematic parameters. This can be solved in a least-squares sense. The solution yields the absolute calibration information required for conventional calibration. However, as mentioned in the Conclusions, novel alternative *relative calibration* approaches will be examined.

The reconstructed sections may also be improved by refining the camera calibration. For this experiment it was deemed sufficient to use a MATLAB GUI and mouse to select four grid points to establish the calibration transformation discussed in Section 2.4. The calibration grid itself was a piece of *Kollegblock* ruled paper. The accuracy can be improved by using a precision grid and selecting the image points with a suitable COG algorithm [7].

In addition to camera calibration, the laser light plane itself must be calibrated for orientation and linearity. This can be accomplished by projecting the laser light plane onto a 4-post calibration object. Comparing the resulting 4 traces with the theoretically expected values gives rotational offset and allows for a quantification of linearity. An *auto-collination* setup may also be considered.

Now that we have established the *proof of principal* of the procedure, the next step is to develop a parametric model for a planar cross section so that we can seamlessly connect overlapping segments. This could be done by knotting together NURBS curve representations of the individual segments. Work is currently being done in this direction.

Finally, we must establish optimal start configurations and motion planning. This comes as the last step because it will not affect the accuracy of the measurements, but will enhance the efficient operation of the system in a production environment.

Bibliography

[1] M. Leitner, J. Hayes, R. Ofner, and C. Sallinger. Repeatability of Industrial Robots. Technical report, Department of Automation, University of Leoben, 2000.

[2] J.M. Hollerbach and C.W. Wampler. The Calibration Index and Taxonomy for Robot Kinematic Calibration Methods. *The International Journal of Robotics Research*, pages 573–591, Vol. 15, 1996.

[3] B.W. Mooring, Z.S. Roth, and M.R. Driels. *Fundamentals of Manipulator Calibration*. Interscience, John Wiley & Sons, New York, N.Y., U.S.A., 1991.

[4] C.H. An, C.G. Atkeson, and J.M. Hollerbach. *Model-based Control of a Robot Manipulator*. The MIT Press, Cambridge, Mass., U.S.A., 1988.

[5] M. Vincze, J.P. Prenniger, and H. Gander. A Laser Tracking System to Measure Position and Orientation of Robot End Effectors Under Motion. *The International Journal of Robotics Research*, pages 305–314, Vol. 13, No. 4, Aug. 1994.

[6] R. Ofner. *Three-Dimensional Measurement via the Light-Sectioning Method*. PhD thesis, Institut für Automation, Montanuniversität Leoben, March, 2000.

[7] R. Ofner, P. O'Leary, and M. Leitner. A Collection of Algorithms for the Determination of Construction Points in the Measurement of 3D Geometries via Light-Sectioning. *Wesic '99, 2nd Workshop on European Scientific and Industrial Collaboration promoting: Advanced Technologies in Manufacturing, Newport, South Wales, United Kingdom*, 1999.

[8] Z. Wu, L. Wu, and A. Wu. The Robost Algorithms for Finding the Center of an Arc. *Computer Vision and Image Understanding*, pages 269–278, Vol. 62, No. 3, November 1995.

[9] M.E. Mortenson. *Geometric Modelling*. John Wiley & Sons, New York, N.Y., U.S.A., 1985.